Adsorption and Thermal Decomposition of Methanol on 3d Transition Metal Aluminides: FeAl(110), NiAl, and TiAl

Bor-Ru Sheu and D. R. Strongin*

Department of Chemistry, State University of New York at Stony Brook, Stony Brook, New York 11794

Received: April 13, 1993; In Final Form: July 2, 1993®

The adsorption and thermal decomposition of methanol on FeAl(110), polycrystalline NiAl, and polycrystalline TiAl have been investigated. Temperature-programmed desorption (TPD) and ultraviolet and X-ray photoelectron spectroscopies (UPS and XPS) are used to investigate the electronic structure and thermal decomposition reactions on 3d transition metal aluminide surfaces. Methane and hydrogen are the two primary products that result from methanol decomposition on all the 3d transition metal aluminides. UPS of CH_3OH/FeAl(110) and CH_3OH/NiAl at 200 and 270 K, respectively, supports the existence of a methoxy intermediate (CH_3O) on the Al component of FeAl(110) and NiAl. XPS results support a surface picture that has carbon chemisorbing on "transition metal" sites and the oxygen remaining on Al during the decomposition of the intermediate species. The peak temperatures of methane desorption from TiAl, FeAl(110), and NiAl are 450, 550, and 590 K, respectively.

1. Introduction

Bimetallic surface chemistry plays a role in many technologically important areas, including catalysis, microelectronics fabrication, electrochemistry, corrosion passivation, and structural materials.[1,2] Aluminides, such as TiAl, FeAl, and NiAl, present a class of bimetallic alloys characterized by a long-range bulk order that is maintained to temperatures near their melting point. Transition metal aluminides then serve as excellent model surfaces for the study of elementary catalytic reactions on bimetallic catalysts, since their surface composition and geometric structure can be well controlled. Furthermore, these aluminide surfaces have many interesting properties that are not present for the corresponding separate transition metal and aluminum crystal surfaces.[3-18]

FeAl and NiAl crystallize in the body-centered CsCl structure, and TiAl adopts a tetragonal crystal structure. Recent analysis of low-energy electron diffraction (LEED) *I-V* curves of FeAl(100) shows that the outermost layer of FeAl(100),[10] similar to NiAl(100),[9] is predominantly Al terminated. Unlike FeAl(100), which can be terminated by all Fe or Al atoms, the ideal FeAl(110) surface contains equal amounts of both constituents. While FeAl(110) has not been investigated by LEED, it might be expected to have a similar surface structure as NiAl(110), which has a rippled structure[11] with the Al surface atoms displaced toward vacuum.

In this research, the thermal decomposition reactions of the catalytically important methanol molecule on three aluminide surfaces are investigated. Extensive studies of the adsorption and decomposition of methanol on 3d transition metals[19-51] and pure Al[52-57] have already been carried out in previous research. These past studies of the elemental systems provide a database that allows a comparison between the 3d transition metal aluminides and the corresponding transition metal and aluminum systems.

On many surfaces the decomposition of methanol led to the production of gaseous hydrocarbon products, such as methane, methanol, and formaldehyde (O/Cu,[40-50] O/Ag,[58] Mo-C,[59,60] W-C[61]). Methanol decomposition on Ni,[19-35] Fe,[36-39] Cr,[51] Ru,[57] Rh,[62-65] Pd,[66-69] and Pt[70-72] results in the formation of adsorbed carbon monoxide and atomic hydrogen. In contrast, methanol decomposition on Ti,[40] W,[59,60] and Mo[61] primarily leads to adsorbed carbon, oxygen, and hydrogen. On aluminum surfaces, methanol decomposition results in methane formation and adsorbed carbon and oxygen.[52-57] The absence of oxygenated gaseous products for aluminum is in contrast to the CO and H_2 production on nickel and iron surfaces. The accepted mechanism for methanol decomposition on most clean metal surfaces involves a methoxy intermediate (CH_3O), which has been spectroscopically identified on many surfaces including Ni,[21,23,28,31,34] Fe,[36,38] Ti,[40] and Al.[53,54,56]

Our research of the reactions of methanol on FeAl(110), polycrystalline NiAl, and polycrystalline TiAl uses ultraviolet photoelectron spectroscopy (UPS), X-ray photoelectron spectroscopy (XPS), and temperature-programmed desorption (TPD). By investigating a series of aluminide surfaces, we show that the contribution of the Al and transition metal component toward methanol surface reactions can be resolved. At the methanol coverages used in this research, the aluminide surface chemistry and product selectivity are dominated by the "aluminum" sites with more subtle contributions from the transition metal component. Photoelectron spectroscopy suggests that a methoxy intermediate exists on FeAl(110), NiAl, and TiAl and that this intermediate preferentially resides on the Al component.

2. Experimental Section

Experiments were performed in a stainless steel ultrahigh-vacuum (UHV) system with a base pressure of 2×10^{-10} Torr (ion and turbomolecular pumped). The chamber is equipped with a quadrupole mass spectrometer (QMS; UTI, Model 100C), LEED optics, double-pass cylindrical mirror analyzer (CMA), X-ray source, differentially-pumped ultraviolet source, and an ion gun. The QMS and CMA were controlled with computer-automated measurement and control (CAMAC) modules interfaced to an IBM-386 computer. XPS and UPS data were obtained by using Mg Kα (1253.6 eV) and He I (21.2 eV) radiation, respectively. The pass energy of photoelectrons through the CMA was set at 50 eV for XPS and 10 eV for the UPS measurements. The energy scale for XPS was obtained by aligning the $2p_{3/2}$ level of a pure Fe sample to 706.8 eV[73] below the Fermi level (E_F).

The FeAl(110) crystal (diameter 1 cm; thickness 0.2 cm) used in this research was spark-cut from a larger single crystalline ingot, and it was subsequently polished by standard metallurgical methods. Laue back-diffraction was used to orient the crystal to within 1.0° of the desired angle. The bulk composition of the

* To whom correspondence should be addressed.

® Abstract published in *Advance ACS Abstracts*, September 1, 1993.

0022-3654/93/2097-10144$04.00/0

ingot was quoted by the supplier (General Electric) to be 40 atomic percent (at. %) Al and 0.02 at. % Zr. Analysis of the Fe($2p_{3/2}$) and Al(2s) XPS peak areas, and using the appropriate sensitivity factors, however, yielded a near-surface composition of 46 at. % Al. Furthermore, by using X-ray diffraction, we determined the lattice constant for this alloy to be 2.904 Å (compared to 2.908 Å for 50 at. % Al FeAl).[74] This lattice constant corresponds well to an FeAl alloy containing 46 at. % Al,[74] and this result is consistent with the XPS result. Only carbon and oxygen contaminations were detected by Auger electron spectroscopy (AES) and XPS on the sample, when initially introduced into the UHV chamber. Cleaning of FeAl(110) was accomplished by repeated cycles of 500-eV argon ion sputter and anneal (at 1073 K for 8 min and at 1173 K for 2 min) cycles. A rectangular (1 × 1) LEED pattern was obtained for FeAl(110) after this cleaning procedure.

Polycrystalline TiAl (0.8 cm^2, thickness 0.2 cm) had a bulk composition of 52 at. % Al, as determined by the supplier (General Electric). Main contaminants in the sample prior to cleaning were carbon and oxygen. TiAl was cleaned by successive 2-keV argon ion sputter and anneal (1273 K, 5 min) cycles. NiAl, supplied by Oak Ridge National Laboratory, had a bulk composition of 50 at. % Al. This sample (0.8 × 0.5 cm rectangle; thickness 0.2 cm) was cleaned by 2-keV argon ion sputter and anneal cycles (1073 K, 10 min). Carbon was removed from NiAl by heating in 1×10^{-7} Torr of oxygen at 1000 K, and the resulting oxygen was removed by the sputter cycles.

Aluminide samples were mounted on a liquid nitrogen cryostat with cooling capabilities down to 120 K. Tantalum support wire was spot-welded to the edges of the samples, and a chromel–alumel (type K) thermocouple wire was spot-welded to the bottom of the sample. TPD experiments were performed with a heating rate of 7 K/s. The QMS was multiplexed so that 10 ions could be monitored during TPD, but typically 5 *m/e* values were monitored, once the product distribution was confirmed for each surface. To facilitate dosing, a 0.05-cm-diameter dosing tube was used to admit the methanol into the UHV chamber, and it was typically 1 cm away from the center of the samples. Methanol (CH_3OH and CH_3OD, >99.5 atom % D; Sigma Chemical Co.) was purified by freeze–pump–thaw cycles. The methanol exposures quoted in this paper are in langmuirs (1 langmuir = 10^{-6} Torr·s), but it is important to note that they are uncorrected for the line-of-sight setup and for the cracking efficiencies of molecules in the ion gauge used for pressure measurements. The actual exposures are expected to be higher than those quoted in the paper. Also, the exposure at the sample surface was very sensitive to the sample–doser distance. Changing samples altered this distance, due to monitoring differences and thus, a comparison of desorption yields between different surfaces was not performed in this research.

3. Results

3.1. Temperature-Programmed Desorption. TPD results are presented individually for all three surfaces used in this research. The first figure for each surface summarizes the products and desorption temperatures at a specified methanol coverage. Subsequent figures for FeAl(110) and NiAl investigate the effect of coverage on the product distribution and desorption temperature. TPD experiments using partially deuterated methanol (CH_3OD) also are presented for the FeAl(110) surface.

3.1.1. CH_3OH/FeAl(110). Figure 1 shows the thermal desorption of H_2 (*m/e* 2), CH_4 (*m/e* 16), CO (*m/e* 28), and CH_3OH (*m/e* 31) from FeAl(110), after a 0.4-langmuir CH_3OH exposure. Figures 2 and 3 monitor the CH_4 and H_2 product as a function of methanol exposure, respectively. A broad CH_4 desorption peak at 550 K and two H_2 desorption peaks with peak temperatures of 300 and 440 K are observed at all methanol exposures.

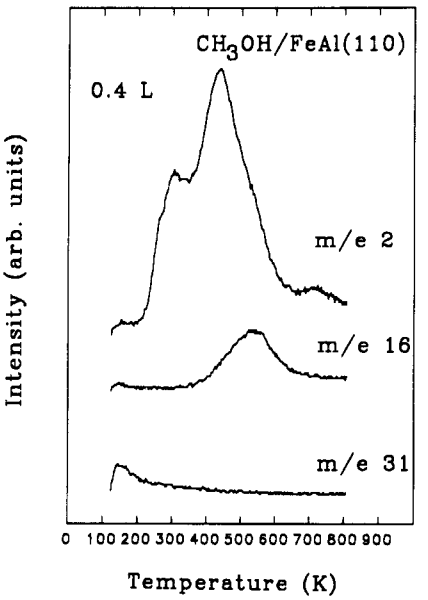

Figure 1. TPD of H_2 (*m/e* 2), CH_4 (*m/e* 16), and CH_3OH (*m/e* 31) from FeAl(110) after a 0.4-langmuir CH_3OH exposure.

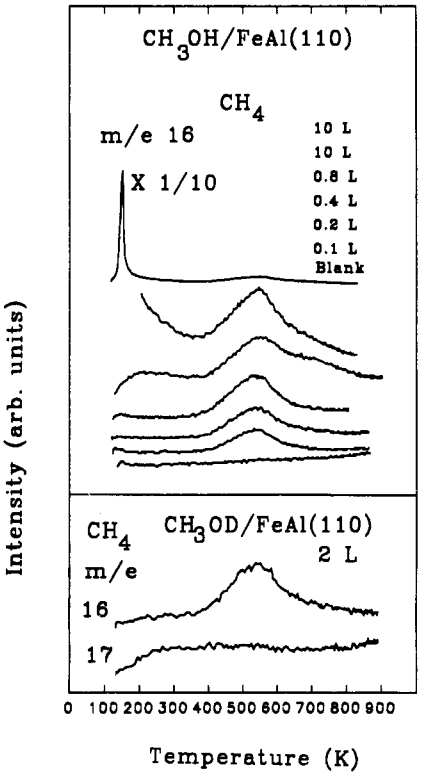

Figure 2. Desorption of CH_4 product from FeAl(110) after exposure to CH_3OH and CH_3OD. The sharp feature at about 150 K in the top panel at 10-langmuir exposure is due to methanol desorption from a condensed layer. In the lower panel, *m/e* 16 and 17 fragments are used to monitor desorption of CH_4 and CH_3D, respectively. No incorporation of the deuterium atom into the methane product is detected.

The bottom panel of Figure 2 shows the thermal desorption of CH_4 and CH_3D from a FeAl(110) surface after a 2-langmuir CH_3OD exposure. Figure 2 shows that CH_4 is produced and that CH_3D is not formed during the decomposition of CH_3OD on FeAl(110).[75] The lower panel of Figure 3 shows the desorption of D_2, H_2, and HD from FeAl(110), after a 2-langmuir CH_3OD exposure. The low-temperature feature in the hydrogen desorption spectrum contains the majority of the deuterium signal. Contributions from dissociation of the CH_3 group in the methanol molecule and the presence of residual hydrogen on FeAl(110) may account for the desorption of H_2 and HD at these

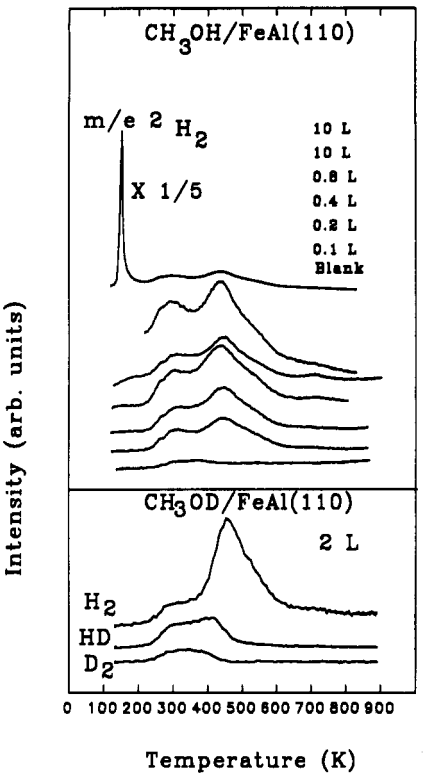

Figure 3. H_2 desorption spectra of CH_3OH/FeAl(110) are shown in the upper panel. Desorption spectra of H_2, HD, and D_2 for CH_3OD/FeAl(110) are shown in the lower panel. D_2 desorbs at a lower temperature than CH_4, consistent with the absence of CH_3D product during CH_3OD decomposition. The sharp peak near 150 K in the 10-langmuir spectrum is due to methanol desorption from a condensed layer.

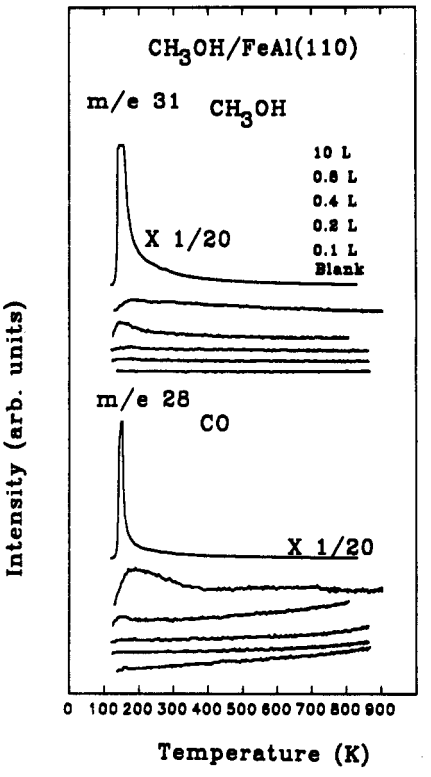

Figure 4. CH_3OH (m/e 31) and CO (m/e 28) desorption spectra of CH_3OH/FeAl(110). The contribution of methanol cracking fragments to the 0.8-langmuir m/e 28 spectrum is small compared to the CO contribution.

temperatures. However, the experiment shows that the desorption of the deuterium molecules occurs before methane desorbs from the FeAl(110) surface. This result is consistent with the absence of deuterium in the methane product. The hydrogen desorption state with a peak temperature of 440 K is then attributed to hydrogen, resulting from the dehydrogenation of the CH_3 group.

Thermal desorption spectra of CH_3OH (m/e 31) and CO (m/e 28), as a function of methanol exposure, are shown in Figure 4. Perhaps the most important aspect of this figure is the evolution of CO (peak maximum near 200 K) at a methanol exposure of 0.8 langmuir. This is evidenced by noting that the m/e 28 intensity is less than that of m/e 31 for lower methanol exposures, but at 0.8 langmuir the m/e 28 intensity becomes substantially greater than the m/e 31 intensity. These data suggest that at higher methanol exposures some oxygenated product can desorb from FeAl(110). We point out here that detailed experiments that can accurately determine the methanol coverage required to produce CO have not been performed.

3.1.2. CH_3OH on Polycrystalline NiAl and TiAl. Figure 5 shows desorption spectra for NiAl after a 0.6 L-CH_3OH exposure. Methane (m/e 16) and hydrogen (m/e 2) are the dominant products with carbon monoxide (m/e 28) being a relatively minor contribution. TPD spectra of methanol and methane, as a function of CH_3OH exposure, are shown in Figure 6. Methane desorption spectra show two desorption states, with peak temperatures of 380 and 590 K. Methanol shows a broad desorption spectrum up to an exposure of 0.12 langmuir. At higher exposures a sharp peak centered at about 150 K evolves, presumably due to methanol desorption from a condensed layer. Also, the methane yield is constant above a methanol exposure of 0.12 langmuir, consistent with this exposure being the point at which multilayers of methanol begin to form.

The desorption spectra of H_2 (Figure 7) are complex with multiple desorption states between 300 and 800 K. The inset to the figure compares the desorption spectrum of hydrogen, resulting

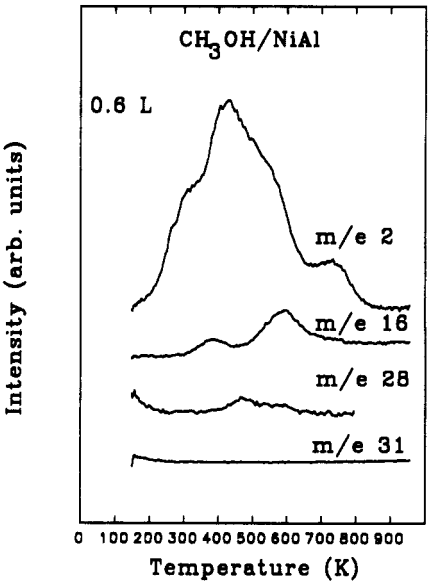

Figure 5. Thermal desorption of H_2 (m/e 2), CH_4 (m/e 16), CO (m/e 28), and CH_3OH (m/e 31) from NiAl after a 0.6-langmuir CH_3OH exposure.

from methanol decomposition, to a spectrum obtained by dosing clean NiAl with molecular hydrogen.[3] The figure shows that the low-temperature shoulder (at 300 K) of the CH_3OH/NiAl spectrum appears at a similar temperature as the hydrogen desorption peak of the H_2/NiAl spectrum. The hydrogen responsible for this desorption state probably results from cleavage of the O–H bond on NiAl at temperatures lower than 300 K, in analogy to the low-temperature hydrogen desorption peak of CH_3OH/FeAl(110). The higher-temperature desorption features (>300 K) are attributed to hydrogen resulting from the dehydrogenation of the CH_3 group of the methanol molecule.

Desorption spectra of CO product are shown in Figure 8, and in contrast to FeAl(110) the desorption of CO is observed at all

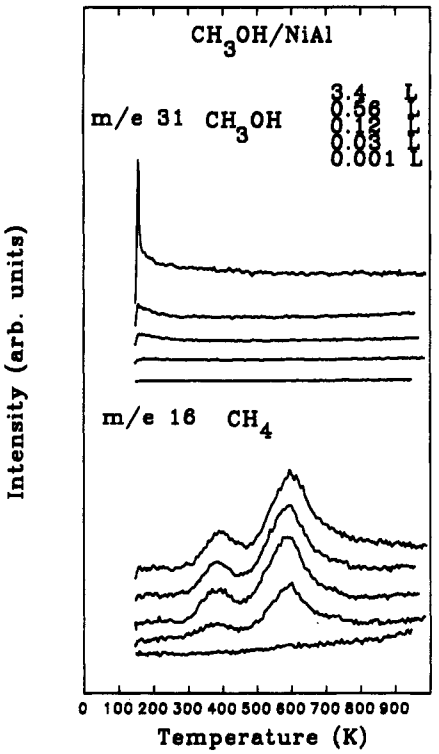

Figure 6. CH_3OH (m/e 31) and CH_4 (m/e 16) desorption from NiAl as a function of CH_3OH exposure.

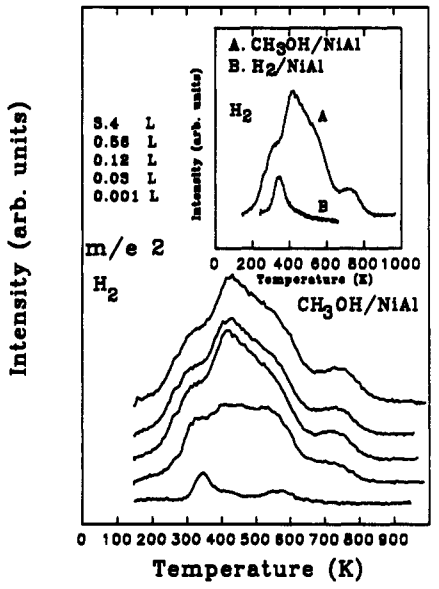

Figure 7. H_2 desorption spectra of CH_3OH/NiAl as a function of CH_3OH exposure. The inset shows the thermal desorption of H_2 from CH_3OH/NiAl and H_2/NiAl.

methanol exposures. Note that the desorption peak below 200 K in the m/e 28 spectra is due to the cracking of desorbing methanol. The inset to the figure compares the CO desorption spectrum obtained from methanol dosed NiAl to one obtained by dosing clean NiAl with 2 langmuirs of CO.[76] The TPD spectrum for CO/NiAl shows that the majority of CO desorbs from NiAl by 400 K. CO produced on NiAl, via the decomposition of methanol, shows desorption at higher temperatures. This comparison suggests that the decomposition reactions of methanol, which produce CO product, occur at temperatures above 400 K.

Figure 9 shows products that desorb from TiAl after a 0.6-langmuir CH_3OH exposure. The desorption curves are representative of a saturation exposure of methanol and show that both H_2 and CH_4 are products. No evidence for CO production (or other oxygenated products) was obtained during our TPD

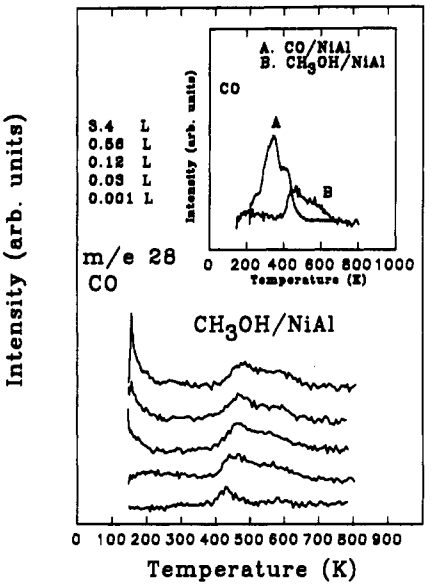

Figure 8. Thermal desorption of CO from NiAl as a function of CH_3OH exposure. The inset shows TPD spectra of CO desorbing from CH_3OH and CO-dosed NiAl surfaces. CO desorbs at a higher temperature when it results from the decomposition of methanol.

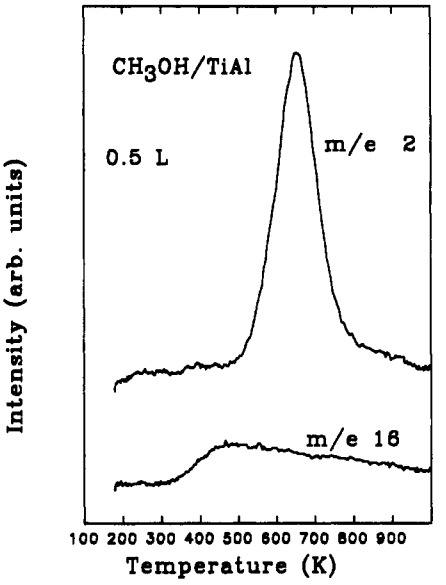

Figure 9. TPD spectra showing that H_2 (m/e 2) and CH_4 (m/e 16) are evolved when CH_3OH decomposes on polycrystalline TiAl.

work on TiAl. The maximum rate of CH_4 and H_2 desorption occurs at 450 and 650 K, respectively.

3.2. UPS. *3.2.1. CH_3OH/FeAl(110).* Valence band measurements of the clean and methanol dosed (4 langmuirs) FeAl(110) surface at 120 K are shown in Figure 10. Also shown are spectra at higher temperatures, which are obtained by heating the surface to the indicated temperature momentarily and then cooling to 120 K. The top panel exhibits difference spectra (dosed surfaces – clean surface), and the bottom panel shows corresponding unprocessed data. A 4-langmuir exposure of CH_3OH at 120 K causes formation of a methanol multilayer on FeAl(110), as judged by TPD experiments that show a sharp desorption peak at 150 K, characteristic of condensed methanol. Gas-phase orbital assignments (referenced to the vacuum level) for methanol are shown at the top of the figure. We have aligned the gas-phase spectrum with the surface bound species in the 120 K spectrum by assuming that the deeper (5a′) and (1a″ + 6a′) orbitals of methanol are least perturbed by any surface bond formation.[54] The structure of the 120 K spectrum is similar to the photoionization spectra of gas-phase methanol, consistent

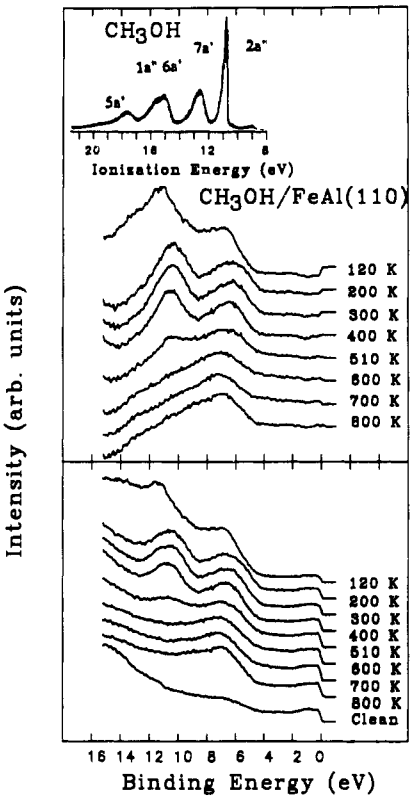

Figure 10. UPS spectra of CH_3OH/FeAl(110) as a function of temperature. The surface is initially dosed with 4 langmuirs of CH_3OH at 120 K and then heated momentarily to the indicated temperatures. The top panel exhibits difference spectra, and the bottom panel shows the raw data. The gas-phase photoelectron spectrum of CH_3OH is shown at the top of the figure (see text for referencing procedure).

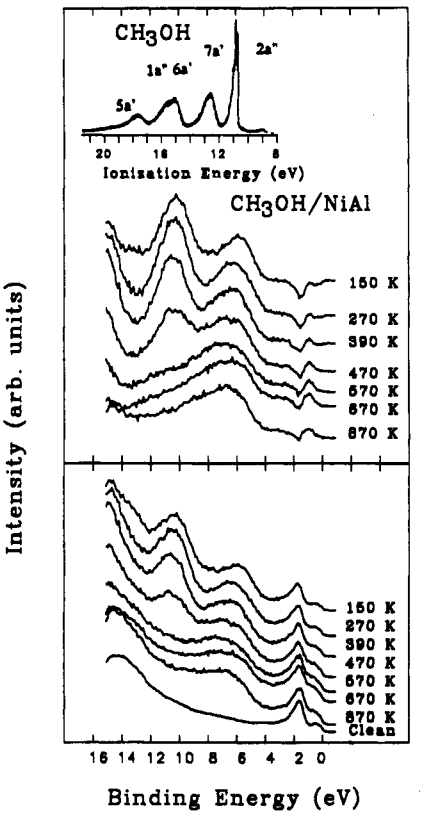

Figure 11. UPS spectra of CH_3OH/NiAl at selected temperatures. The NiAl surface is initially dosed with 2 langmuirs of CH_3OH at 150 K. The top panel exhibits difference spectra, and the bottom panel shows raw data. The gas-phase photoelectron spectrum of CH_3OH is shown at the top of the figure (see text for referencing procedure).

with the presence of condensed methanol. After heating the methanol layer to 200 K, the valence band spectrum changes to one consisting of two broad features having intensity maxima at 6.4 and 10.4 eV. This 200 K spectrum is similar to the photoemission valence band spectra of methoxy species, CH_3O-(ads), on other surfaces.[34,40,51,54] Therefore, we postulate that methoxy species exist on FeAl(110) at 200 K. Using the methanol orbital notation, the 6.4- and 10.4-eV features are assigned to the (2a″ + 7a′) and (6a′ + 1a″ + 5a′) orbitals of methoxy, respectively.[34,49,51] The 10.4-eV feature, which is associated with the C–O bond and methyl group in the methoxy species, shows a small decrease in intensity upon heating to 400 K. However, on the basis of the 400 K spectrum, we conclude that most of the methoxy is stable at 400 K. Further heating to 510 K markedly reduces the intensity of the high binding energy feature, and at 600 K this feature has been eliminated. A broad peak remains in the spectra near 7 eV, upon heating to 800 K, and this feature is assigned to surface oxygen. These data show that substantial decomposition of methoxy on FeAl(110) occurs between 400 and 510 K, and the fragmentation is complete by 600 K. TPD results are consistent with these UPS data, since the majority of gaseous decomposition products (i.e., hydrogen and methane) desorb between 400 and 600 K. We stress from the onset that our identification of the methoxy species is based on the similarity of our photoelectron spectroscopy results with those obtained in past studies. Vibrational spectroscopy experiments will be performed in the future, in our laboratory, to better characterize these surface intermediates.

3.2.2. CH_3OH/NiAl. Figure 11 shows valence band spectra of clean and methanol dosed NiAl as a function of temperature. Exposure of NiAl to 2 L-CH_3OH at 150 K produces two broad peaks at 6.0 and 10.2 eV below E_F. These features are assigned to the (2a″) and (1a″ + 6a′) molecular orbitals of methanol. Also present are smaller peaks at 8 and 13 eV, and these features are assigned to the (7a′) and (5a′) orbitals of methanol. Heating CH_3OH/NiAl to 270 K leaves only two broad peaks at 6.4 and 10.4 eV. As was done in the FeAl(110) circumstance, these levels are assigned to those of the methoxy species (i.e., 2a″ + 7a′ and 6a′ + 1a″ + 5a′ orbitals). Therefore, the binding energies of the valence features of the surface intermediate species are 6.4 and 10.4 eV on both FeAl(110) and NiAl. Heating the CH_3OH/NiAl surface to 390 K leaves the valence band spectrum relatively unchanged. Further heating to 470 K significantly reduces the intensity of the higher binding energy peak, and this feature is barely above background in the 570 K spectrum. The high binding energy peak is completely eliminated in the 670 K spectrum, leaving only a feature due to atomic oxygen (also present in the 870 K spectrum). These results suggest that a significant fraction of methoxy dissociates between 390 and 470 K (presumably through both dehydrogenation steps and C–O bond breaking), and decomposition is complete at temperatures between 570 and 670 K. TPD spectra of CH_3OH/NiAl show CH_4, H_2, and CO desorption in this same temperature range.

3.3. XPS of CH_3OH/FeAl(110), CH_3OH/NiAl, and CH_3OH/TiAl. XPS O(1s) and C(1s) spectra of the 4-langmuir CH_3OH/FeAl(110), 2-langmuir CH_3OH/NiAl, and 2-langmuir CH_3OH/TiAl systems at various temperatures are shown in Figure 12. The adsorption temperature of CH_3OH on FeAl(110), NiAl, and TiAl is 120, 150, and 160 K, respectively. Spectra corresponding to higher temperatures are obtained by heating the surface to the indicated temperature momentarily and then cooling back to the adsorption temperature. Vertical dashed lines in the O(1s) and C(1s) spectra are aligned to 532.4 and 286.4 eV, respectively. The vertical dotted line in the O(1s) spectra corresponds to 531.2 eV. Vertical dotted lines in the C(1s) spectra for FeAl(110), NiAl, and TiAl are aligned to 282.4, 282.8, and 281.2 eV, respectively.

UPS experiments already presented suggest that methoxy species exist on FeAl(110) and NiAl at 200 and 270 K,

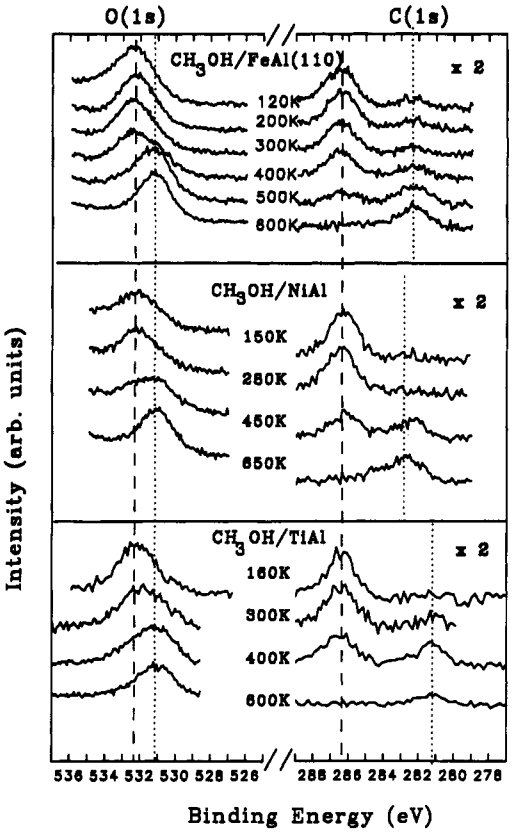

Figure 12. O(1s) and C(1s) XPS spectra of CH_3OH-dosed transition metal aluminides after heating to various temperatures. The vertical dashed lines in the O(1s) and C(1s) spectra are aligned at 532.4 and 286.4 eV, respectively, and are assigned to methoxy species. Decomposition of this surface intermediate shifts the O(1s) level to 531.2 eV for all the aluminides, and this energy position is marked by the vertical dotted line. The C(1s) binding energy (vertical dotted line energy position), after methoxy decomposition, depends on whether Fe, Ni, or Ti is present.

TABLE I: O(1s) and C(1s) Binding Energies (eV), Relative to E_F, of Methoxy Species on Various Surfaces

surface	O(1s)	C(1s)	ref
Al(poly)[a]	532.7	287.1	54
Si(111)	532.8	287.0	77
Rh(111)	532.0	285.7	78
Fe(100)	531.2	285.4	39
Pd(111)		285.9	79
FeAl(110)	532.4	286.4	this work
NiAl(poly)[a]	532.4	286.4	this work
TiAl(poly)[a]	532.4	286.4	this work

[a] The abbreviation poly denotes polycrystalline surface.

respectively. Therefore, we assign the O(1s) and C(1s) features at 532.4 and 286.4 eV, respectively, in the 200 K FeAl(110) and 280 K NiAl spectra to methoxy species. Furthermore, these O(1s) and C(1s) binding energies are consistent with the corresponding levels of methoxy on metal surfaces (see Table I), supporting our contention that methoxy exists on FeAl(110) and NiAl.

Heating CH_3OH/FeAl(110) and CH_3OH/NiAl to 600 and 650 K, respectively, causes a shift of the O(1s) binding energy, for both surfaces, from 532.4 to 531.2 eV, as shown by the spectra in Figure 12. Corresponding C(1s) spectra show that this increase in temperature results in the elimination of the 286.4-eV feature and the appearance of peaks at 282.4 and 282.8 eV in the 600 K FeAl(110) and 650 K NiAl spectrum, respectively. We attribute these O(1s) and C(1s) binding energy changes to the thermal decomposition of methoxy species into atomic oxygen and carbon (or partially hydrogenated species). On the basis of C(1s) peak areas, it is estimated that 40% of the surface carbon desorbs when CH_3OH/FeAl(110) is heated from 200 to 600 K. A similar analysis estimates that 40% of the carbon leaves the near surface region when CH_3OH/NiAl is heated from 280 to 650 K. This decrease in surface carbon is attributed to the desorption of methane from FeAl(110) and NiAl. The diffusion of carbon into the bulk or the surface segregation of aluminum,[3,14,15] which will attenuate the C(1s) photoelectrons, during heating cannot be ruled out by these data. An analysis of the O(1s) data indicates that, within experimental error, surface oxygen does not decrease by a measurable amount when CH_3OH/FeAl(110) and CH_3OH/NiAl are heated to 600 and 650 K, respectively. This result suggests that the desorption of CO is a minor reaction pathway compared to the formation of methane. While not shown here, heating to 800 K does not lead to any significant changes in the O(1s) and C(1s) spectra.

The 160 and 300 K CH_3OH/TiAl spectra show O(1s) and C(1s) features at 532.4 and 286.4 eV, respectively. The 300 K spectrum also shows a feature appearing on the low-energy side of the 532.4-eV O(1s) peak and the growth of a C(1s) feature at 281.2 eV. These data suggest that some decomposition of surface species on TiAl occurs upon heating to 300 K. We do not have corresponding UPS data for the TiAl surface to better identify the surface intermediate. However, the similarity of the photoelectron features at 532.4 and 286.4 eV in the TiAl spectra to those in the 200 K FeAl(110) and 280 K NiAl spectra suggest that methoxy species also exist on TiAl. It is noted that the 600 K O(1s) spectrum shows a decrease in O(1s) intensity, relative to data at lower temperatures. We attribute this decrease to oxygen dissolving into the TiAl bulk, since no oxygenated products are observed desorbing from TiAl during TPD experiments. It is estimated from the C(1s) peak areas that 80% of the carbon leaves the near surface region when the CH_3OH/TiAl surface is heated from 300 to 600 K. This value is much higher than that obtained for the FeAl(110) and NiAl surfaces. We attribute a significant portion of the C(1s) decrease, for the TiAl surface, to diffusion into the bulk. Diffusion of carbon and oxygen into the bulk at these temperature is consistent with previous research that showed that oxygen and carbon (from CO dissociation) diffuses into pure Ti at temperatures between 573 and 773 K.[80]

Comparing all the systems shows that decomposition of methoxy on FeAl(110), NiAl, and TiAl shifts the O(1s) binding energy from 532.4 to 531.2 eV. In contrast, the difference between the C(1s) binding energy of methoxy (vertical dashed line) and of its decomposition fragment (vertical dotted line), at 600 K or higher, depends on the nature of the transition metal component. For example, the C(1s) binding energy differences are 4.0, 3.6, and 5.2 eV for methoxy decomposition on FeAl(110), NiAl, and TiAl, respectively. Therefore, the magnitude of the C(1s) shift depends on whether Fe, Ni, or Ti is present, and the shift of the O(1s) level is independent of the transition metal. It is emphasized that the C(1s) features, which appear below 283 eV on the aluminides, are representative of carbonaceous species that presumably do not react to form methane. These XPS results support a surface picture that has the oxygen chemisorbing on "Al" sites and carbon primarily bonding to "transition metal" sites during methoxy decomposition on the aluminides. Further support of this picture is obtained by comparing the O(1s) and C(1s) binding energies of the dissociation fragments on FeAl(110) and TiAl to those obtained for Fe, Ti, and Al surfaces. For example, the O(1s) binding energy of oxygen on aluminum is typically between 531.0 and 531.5 eV,[81,82] while the O(1s) binding energy of oxygen on Fe[83] and Ti[80] is close to 530.0 eV. Furthermore, the C(1s) binding energy of adsorbed carbon is typically near 282.0 on Fe[83] and closer to 281.5 eV on Ti.[80] Decomposition of methoxy on FeAl(110) leads to O(1s) and C(1s) energies of 531.2 and 282.4 eV, respectively. The corresponding binding energies after methoxy decomposition on TiAl are 531.2 and 281.2 eV. Therefore, these binding energy values, obtained after methoxy decomposition on FeAl(110) and TiAl, are

consistent with a surface picture that has oxygen on aluminum and carbon on transition metal.

4. Discussion

4.1. Product Distribution. TPD experiments show that CH_4 and H_2 dominate the product distribution for all three aluminide surfaces. It has been shown conclusively in previous research that methanol decomposition on nickel and iron surfaces results in the desorption of CO and H_2.[19-39] The chemistry of methanol on Al is in stark contrast to Fe and Ni surfaces, in that oxygenated products are not produced during the thermal decomposition of the methanol molecule. Instead, the evolution of gaseous CH_4 and H_2 are observed, and all the oxygen from the methanol molecule remains on the Al surface.[52-57] Comparison of the product distribution for the aluminides to those of the aluminum and transition metal systems shows that the Al component of NiAl and FeAl exerts a strong influence on the gaseous product distribution. The strong Al–O interaction presumably favors the production of methane over oxygenated products.

TPD experiments show that some CO desorbs from FeAl(110), after a relatively high exposure to methanol, and from NiAl after all methanol exposures. These results suggest that the transition metal component does have an effect on the product distribution. The formation of CO during methanol decomposition, however, is a minor reaction channel on FeAl(110) and NiAl, compared to CH_4 production. This statement is supported by XPS data, which has shown that the amount of oxygen remains relatively constant, but the amount of surface carbon is significantly reduced when CH_3OH-dosed FeAl(110) and NiAl are heated to 600 and 650 K, respectively. The influence of the transition metal on the details of the bonding on these bimetallic surfaces also is shown by other TPD data, for example, the peak temperature of CH_4 desorption from NiAl > FeAl > TiAl, showing that the transition metal partially controls the surface reactions of the hydrocarbon fragments. This conclusion, based on TPD data, is consistent with XPS data that suggest that carbon-containing species are transferred to the transition metal component, during methanol decomposition reactions. Again, we mention that our XPS results address the adsorption site of the strongly bound carbon component, which forms during methoxy decomposition. The location of the hydrocarbon fragments that react to form methane cannot be directly ascertained from these XPS measurements.

The hydrogen desorption spectra for FeAl and NiAl most likely represent many successive dehydrogenation and desorption steps. A few general comments about the hydrogen product, however, can be constructed from our data. First, as has already been mentioned, the desorption of the hydroxyl-hydrogen from FeAl(110) (and probably NiAl) occurs at a lower temperature than methane production and desorption. Second, the hydrogens desorbing above 400 K from FeAl(110) and NiAl are bound in organic fragments immediately preceding desorption, since atomic hydrogen on NiAl and FeAl would combine and desorb as molecular hydrogen at lower temperatures.[3] Third, desorption of hydrogen from TiAl after methanol decomposition results in a single high temperature peak at 650 K. Desorption of hydrogen from a TiAl surface after an exposure to molecular hydrogen also occurs near 650 K.[3] Therefore, in contrast to FeAl(110) and NiAl, the decomposition of organic fragments on TiAl to adsorbed carbon and hydrogen occurs at temperatures below where H_2 can desorb from the surface.

4.2. Methoxy Adsorption. Table II summarizes the binding energies of the valence band features of methoxy determined in this research of the aluminides and in previous research of pure metal surfaces. (Data for iron are not available.) Note that the 4a′ feature lies too deep to be probed by UPS with the He I line (21.2 eV). Table II shows that for the pure metal surfaces the binding energies of the methoxy levels (labeled in the methanol orbital notation)[34,49,51] depend on the adsorbing element. One might expect that if methoxy species were adsorbing primarily on the transition metal component of the aluminides, there would be significant differences between the binding energies of the valence band features for FeAl(110) and NiAl. The binding energies of the methoxy valence band features on FeAl(110), however, are very similar to the corresponding levels on NiAl. Therefore, our results suggest that most of the methoxy resides on the "aluminum" sites of FeAl(110) and NiAl. The high affinity of Al for oxygen (leading to O–H bond scission in CH_3OH), relative to the transition metal, is probably responsible for this selectivity in adsorption site. It is noted that these UPS data (and for the XPS data presented next) show that the binding energies of the methoxy levels are different on the aluminides than on pure Al. These differences may be a result of the modified electronic structure of Al in the aluminide, compared to pure Al.[84]

TABLE II: Binding Energies (eV) of Methoxy Levels Relative to E_F on Various Surfaces

surface	(2a″ + 7a′)	(6a′ + 1a″ + 5a′)	(4a′)	ref
Cu(110)	5.5	8.5	15.5	49
Ni(111)	5.3	9.5	*a*	34
Cr(110)	6.6	10.7	17.3	51
Ti(001)	6.2	10.3	16.8	40
Al(poly)[b]	7.4	11.2	18.4	54
FeAl(110)	6.4	10.4	*a*	this work
NiAl(poly)[b]	6.4	10.4	*a*	this work

[a] Not accessible with He I radiation. [b] The abbreviation poly denotes polycrystalline surface.

Similar to the valence levels, the binding energies of the O(1s) and C(1s) core levels of methoxy (Table I) show significant variations depending on the adsorbing element. Perhaps the most revealing aspect of these data then, is that the O(1s) and C(1s) binding energies of methoxy on FeAl(110), NiAl, and TiAl are similar. These data suggest that there is a common adsorption site for methoxy on the aluminides. Therefore, we again infer from photoemission results that the majority of the methoxy species are bound on "aluminum" sites of FeAl(110), NiAl, and TiAl. The details of the bonding geometry of methoxy cannot be determined from these data. We only infer from the data that methoxy primarily interacts with the Al component of the aluminides. Furthermore, the TPD results are consistent with this contention, since decomposition of the methoxy group results primarily in methane and hydrogen rather than CO, which would be associated with the transition metal.

4.3. Thermal Stability of Methoxy. Methoxy decomposition occurs near 450 K on Al(111)[53] and at slightly lower temperatures (near 400 K) on Fe(110)[38] and Fe(100).[37,39] On Ni(110)[19-24] and Ni(111),[29-35] methoxy decomposes into adsorbed CO and H below 300 K. Both UPS and XPS experiments show that a significant amount of methoxy exists on FeAl(110) and NiAl near 400 K. At higher temperatures these photoelectron techniques show that substantial decomposition of the intermediate occurs on both these bimetallic surfaces. Within the temperature resolution of our experiments, the thermal stability of methoxy on FeAl(110) is similar to its stability on the separate Al and Fe surfaces. Methoxy, however, shows a much greater thermal stability on NiAl than on Ni. This observation is consistent with methoxy residing preferentially on the Al component.

TPD results have shown that the transition metal component has an effect on product desorption temperatures. XPS results for TiAl and FeAl(110) suggest that the transition metal also has an effect on the stability of the methoxy intermediate. Comparison of the 400 K O(1s) spectra (Figure 12) of CH_3OH/FeAl(110) and CH_3OH/TiAl shows that methoxy has decomposed to a greater extent on TiAl than FeAl(110). Furthermore, the peak temperatures of methane desorption from TiAl and FeAl(110)

are 450 and 550 K, respectively. This result also suggests that methoxy decomposition occurs at a lower temperature on TiAl. This comparison should be viewed with some caution because of the polycrystalline nature of the TiAl sample.

5. Summary

The adsorption and thermal decomposition of methanol on FeAl(110), TiAl, and NiAl have been investigated with XPS, UPS, and TPD. TPD experiments show that methanol decomposition on FeAl(110), NiAl, and TiAl leads primarily to methane and hydrogen desorption. Carbon monoxide product also is found to desorb from NiAl after exposure to methanol.

By investigating a series of 3d transition metal aluminides with photoelectron spectroscopies, a surface picture for methanol on these bimetallic surfaces has been developed. UPS and XPS suggest that a methoxy intermediate resides on all the aluminide surfaces below 400 K. The spectroscopic data are consistent with methoxy adsorbing preferentially on the Al component of these bimetallic surfaces. Furthermore, XPS data indicates that, during methoxy decomposition, oxygen resides on Al and carbonaceous species are transferred to the transition metal component.

Acknowledgment. Support of this research by the National Science Foundation through a NSF–Young Investigator Award (NYI) is greatly appreciated (Grant DMR-9258544). We also appreciate Oak Ridge National Laboratory for supplying NiAl samples and General Electric for supplying FeAl and TiAl.

References and Notes

(1) Campbell, C. T. *Annu. Rev. Phys. Chem.* **1990**, *41*, 775.
(2) Rodriguez, J. A; Goodman, D. W. *J. Phys. Chem.* **1991**, *95*, 4196.
(3) Gleason, N. R.; Gerken, C. A.; Strongin, D. R. *Appl. Surf. Sci.*, in press.
(4) Lui, S.-C.; Mundenar, J. M.; Plummer, E. W.; Mostoller, M.; Nicklow, R. M.; Zehner, D. M.; Ford, W. K.; Erskine, J. In *Physical and Chemical Properties of Thin Metal Overlayers and Alloy Surfaces*; Zehner, D. M., Goodman, G. W., Eds.; *Mater. Res. Soc. Symp. Proc.* **1987**, *83*, 47.
(5) Wuttig, M.; Hoffmann, W.; Preuss, E.; Franchy, R.; Ibach, H.; Chen, Y.; Xu, M. L.; Tong, S. Y. *Phys. Rev. B* **1990**, *42*, 5443.
(6) Chen, Y.; Xu, M. L.; Tong, S. Y.; Wuttig, M.; Hoffmann, W.; Preuss, E.; Franchy, R.; Ibach, H. *Phys. Rev. B* **1990**, *42*, 5451.
(7) Kang, M. H.; Lui, S.-C.; Mele, E. J.; Plummer, E. W.; Zehner, D. M. *Phys. Rev. B* **1990**, *41*, 4920.
(8) Lui, S.-C.; Kang, M. H.; Mele, E. J.; Plummer, E. W.; Zehner, D. M. *Phys. Rev. B* **1990**, *39*, 13149.
(9) Davis, H. L.; Noonan, J. R. In ref 4, p 3.
(10) Wang, C. P.; Jona, F.; Gleason, N. R.; Strongin, D. R.; Marcus, P. M. Manuscript in preparation.
(11) Yalisove, S. M.; Graham, W. R. *Surf. Sci.* **1987**, *183*, 556.
(12) Mundener, J. M.; Gaylord, R. H.; Lui, S.-C.; Plummer, E. W.; Seddon, L.; Zehner, D. M.; Ford, W. K. In ref 4, p 59.
(13) Zehner, D. M.; Gruzalski, G. R. In ref 4, p 199.
(14) Jaeger, R. M.; Kuhlenbeck, H.; Freund, H.-J.; Wuttig, M.; Hoffmann, W.; Francy, R.; Ibach, H. *Surf. Sci.* **1991**, *259*, 235.
(15) Isern, H.; Castro, G. R. *Surf. Sci.* **1989**, *211/212*, 865.
(16) Grillo, M. E.; Castro, G. R.; Doyen, G. *J. Chem. Phys.* **1992**, *97*, 7786.
(17) Grillo, M. E.; Castro, G. R.; Doyen, G. *J. Phys.: Condens. Matter* **1992**, *4*, 5103.
(18) Patterson, C. H.; Buck, T. M. *Surf. Sci.* **1989**, *218*, 431.
(19) Vajo, J. J.; Campbell, J. H.; Becker, C. H. *J. Phys. Chem.* **1991**, *95*, 9457.
(20) Vajo, J. J.; Campbell, J. H.; Becker, C. H. *J. Vac. Sci. Technol. A* **1989**, *7*, 1949.
(21) Richter, L. J.; Gurney, B. A.; Villarrubias, J. S.; Ho, W. *Chem. Phys. Lett.* **1984**, *113*, 185.
(22) Richter, L. J.; Ho, W. *J. Chem. Phys.* **1985**, *83*, 2569.
(23) Bare, S. R.; Stroscio, J. A.; Ho, W. *Surf. Sci.* **1985**, *150*, 399.
(24) Richter, L. J.; Ho, W. *J. Vac. Sci. Technol. A* **1985**, *3*, 1549.
(25) Miragliotta, J.; Polizzotti, R. S.; Rabinowitz, P.; Cameron, S. D.; Hall, R. B. *Chem. Phys.* **1990**, *143*, 123.
(26) Johnson, S.; Madix, R. J. *Surf. Sci.* **1981**, *103*, 361.
(27) Hall, R. B.; Desantolo, A. M.; Bares, S. J. *Surface. Sci.* **1985**, *161*, L533.
(28) Baudais, F. L.; Borschke, A. J.; Fedyk, J. D.; Dignam, M. J. *Surf. Sci.* **1980**, *100*, 210.
(29) Gates, S. M.; Russell, J. N.; Yates, J. T., Jr., *J. Catal.* **1985**, *92*, 25.
(30) Gates, S. M.; Russell, J. N.; Yates, J. T., Jr., *Surf. Sci.* **1984**, *146*, 199.
(31) Demuth, J. E.; Ibach, H. *Chem. Phys. Lett.* **1979**, *60*, 395.
(32) Hall, R. B.; Grubb, A. M.; Grubb, S. G. *J. Vac. Sci. Technol. A* **1987**, *5*, 865.
(33) Gates, S. M.; Russell, J. N.; Yates, J. T., Jr., *Surf. Sci.* **1985**, *159*, 233.
(34) Rubloff, G. W.; Demuth, J. E. *J. Vac. Sci. Technol.* **1977**, *14*, 419.
(35) Russell, J. N.; Jr., Chorkendorff, I.; Yates, J. T., Jr., *Surf. Sci.* **1987**, *183*, 316.
(36) Albert, M. R.; Lu, J.-P.; Bernasek, S. L.; Dwyer, D. J. *Surf. Sci.* **1989**, *221*, 197.
(37) Lu, J.-P.; Albert, M. R.; Bernasek, S. L.; Dwyer, D. S. *Surf. Sci.* **1989**, *218*, 1, 49.
(38) McBreen, P. H.; Erley, W.; Ibach, H. *Surf. Sci.* **1983**, *133*, L469.
(39) Benziger, J. B.; Madix, R. J. *J. Catal.* **1980**, *65*, 36.
(40) Hanson, D. M.; Stockbauer, R.; Madey, T. E. *J. Chem. Phys.* **1982**, *77*, 1569.
(41) Lindner, T.; Somers, J.; Bradshaw, A. M.; Kilcoyne, A. L. D.; Woodruff, D. P. *Surf. Sci.* **1988**, *203*, 333.
(42) Ricken, D. E.; Somers, J.; Robinson, A. W.; Bradshaw, A. M. *Faraday Discuss. Chem. Soc.* **1990**, *89*, 291.
(43) Wachs, I. E.; Madix, R. J. *J. Catal.* **1977**, *53*, 208.
(44) Sexton, B. A. *Surf. Sci.* **1979**, *88*, 299.
(45) Sexton, B. A.; Hughes, A. E.; Avery, N. R. *Surf. Sci.* **1985**, *155*, 366.
(46) Holub-krappe, E.; Prince, K. C.; Horn, K.; Woodruff, D. P. *Surf. Sci.* **1986**, *173*, 176.
(47) Ryberg, R. *Phys. Rev. Lett.* **1982**, *49*, 1579.
(48) Russell, J. N.; Jr., Gates, S. M.; Yates, J. T., Jr., *Surf. Sci.* **1985**, *163*, 516.
(49) Bowker, M.; Madix, R. J. *Surf. Sci.* **1980**, *95*, 190.
(50) Andersson, S.; Persson, M. *Phys. Rev. B* **1981**, *24*, 3659.
(51) Shinn, N. D. *Surf. Sci.* **1992**, *278*, 157.
(52) Basu, P.; Chen, J. G.; Ng, L. I.; Colaianni, M. L.; Yates, J. T., Jr. *J. Chem. Phys.* **1988**, *89*, 2406.
(53) Chen, J. G.; Basu, P.; Ng, L.; Yates, J. T., Jr., *Surf. Sci.* **1988**, *194*, 397.
(54) Rogers, J. W.; Jr., Hance, R. L.; White, J. M. *Surf. Sci.* **1980**, *100*, 388.
(55) Tindall, I. F.; Vickerman, J. C. *Surf. Sci.* **1985**, *149*, 577.
(56) Waddill, G. D.; Kesmodel, L. L. *Surf. Sci.* **1987**, *182*, L248.
(57) Hrbek, J.; dePaola, R. A.; Hoffmann, F. M. *J. Chem. Phys.* **1984**, *81*, 2818.
(58) Wachs, I. E.; Madix, R. J. *J. Catal.* **1978**, *76*, 531.
(59) Ko, E. I.; Madix, R. J. *Surf. Sci.* **1981**, *112*, 373.
(60) Miles, S. L.; Bernasek, S. L.; Gland, J. L. *J. Phys. Chem.* **1983**, *87*, 1626.
(61) Ko, E. I.; Benziger, J. B.; Madix, R. J. *J. Catal.* **1980**, *62*, 264.
(62) Chuah, G.-K.; Kruse, N.; Schmidt, W. A.; Block, J. H.; Abend, G., *J. Catal.* **1989**, *119*, 342.
(63) Solymosi, F.; Berko, A.; Tarnoczi, T. I. *Surf. Sci.* **1984**, *141*, 533.
(64) Solymosi, F.; Berko, A.; Tarnoczi, T. I. *J. Chem. Phys.* **1987**, *87*, 6745.
(65) Parmeter, J. E.; Jiang, X.; Goodman, D. W. *Surf. Sci.* **1990**, *240*, 85.
(66) Christmann, K.; Demuth, J. E. *J. Chem. Phys.* **1982**, *76*, 6308, 6318.
(67) Gates, J. A.; Kesmodel, L. L. *J. Catal.* **1983**, *83*, 437.
(68) Kok, G. A.; Noordermeer, A.; Nieuwenhuys, B. E. *Surf. Sci.* **1983**, *135*, 65.
(69) Bhattacharya, A. K.; Chesters, M. A.; Pemble, M. E.; Sheppard, N. *Surf. Sci.* **1988**, *206*, L845.
(70) Sexton, B. A.; Rendulic, K. D.; Hughes, A. E. *Surf. Sci.* **1982**, *121*, 181.
(71) Sexton, B. A. *Surf. Sci.* **1981**, *102*, 271.
(72) Akhter, S.; White, J. M. *Surf. Sci.* **1986**, *167*, 101.
(73) Fuggle, J. C.; Mårtensson, N. *J. Electron Spectrosc. Relat. Phenom.* **1980**, *21*, 275.
(74) Bradley, A. J.; Jay, A. H. *J. Iron Steel Instit.* **1932**, *125*, 339.
(75) CH_2D_2 (*m/e* 18), CHD_3 (*m/e* 19), and CD_4 (*m/e* 20) also did not desorb during TPD. The broad signal between 120 and 500 K in the *m/e* 17 spectrum is due to water desorption. Some of the *m/e* 17 intensity is due to water desorption from the cryostat during TPD. We are uncertain what this contribution is, and hence, any discussion of this product is dubious at this time.
(76) Gleason, N. R.; Strongin, D. R. *Surf. Sci.*, in press.
(77) Tanaka, K.; Matsuzaki, S.; Toyoshima, I. *J. Phys. Chem.* **1993**, *97*, 5673.
(78) Houtman, C.; Barteau, M. A. *Langmuir* **1990**, *6*, 1558.
(79) Levis, R. J.; Zhicheng, J.; Winograd, N. *J. Am. Chem. Soc.* **1989**, *111*, 4605.
(80) Fukuda, Y.; Lancaster, F. M.; Honda, F.; Rabalais, J. W. *J. Chem. Phys.* **1978**, *69*, 3447.
(81) Paparazzo, E. *Appl. Surf. Sci.* **1986**, *25*, 1.
(82) Pashutski, A.; Hoffman, A.; Folman, M. *Surf. Sci. Lett.* **1989**, *208*, L91.
(83) Moon, D. W.; Dwyer, D. J.; Bernasek, S. L. *Surf. Sci.* **1985**, *163*, 215.
(84) Schultz, P. A.; Davenport, J. W. *Scr. Metall.* **1992**, *27*, 629.